S-WAVE SPLITTING FROM RECORDS OF LOCAL MICRO-EARTHQUAKES IN WEST BOHEMIA/VOGTLAND: AN INDICATOR OF COMPLEX CRUSTAL ANISOTROPY

V. VAVRYČUK AND A. BOUŠKOVÁ

Institute of Geophysics, Acad. Sci. Czech Republic, Boční II/1401, 141 31 Praha 4, Czech Republic (vv@ig.cas.cz, ab@ig.cas.cz)

Received: January 12, 2008; Revised: May 29, 2008; Accepted: September 9, 2008

ABSTRACT

Most S-wave particle motions of local micro-earthquakes in the West Bohemia/Vogtland region display S-wave splitting. The split S waves are usually well defined, being separated in time and polarized in roughly perpendicular directions in the horizontal projection. In most cases, the polarization of the fast S wave is aligned NW-SE (referred to as "normal splitting"), which is close to the direction of the maximum horizontal compression in the region. However, for some ray directions, the polarization of the fast S wave is aligned NE-SW (referred to as "reverse splitting"). The pattern of normal/reverse splitting on a focal sphere is station-dependent, indicating the presence of inhomogeneities in anisotropy. For some stations, the normal/reverse splitting pattern is asymmetric with respect to the vertical axis, indicating the symmetry axes of anisotropy are probably inclined. The presence of inclined anisotropy is confirmed by observations of directionally dependent delay times between split S waves. A complex and station-dependent anisotropy pattern is probably the result of a complicated anisotropic crust characterized by diverse geological structures. The spatial variation of anisotropy probably reflects the presence of a variety of different types of anisotropic rocks in the region.

Key words: anisotropy, Earth's crust, earthquake swarm, micro-earthquakes, polarization, stress field, S waves, S-wave splitting, 90º-flips, West Bohemia/Vogtland

1. INTRODUCTION

Seismic anisotropy is a general property of rocks in the Earth's crust and upper mantle (*Babuška and Cara, 1991*; *Savage, 1999*). It affects propagation velocities of seismic waves, their polarization and amplitudes, and complicates wave modelling. Also focal mechanisms of earthquakes are more complex if the source area is anisotropic (*Vavryčuk, 2005, 2006*; *Rössler et al., 2004, 2007*). One of the most frequent and striking phenomena, produced by seismic anisotropy, is S-wave splitting, when one S wave, propagating in an isotropic medium, is split into two S waves if the medium is anisotropic (*Crampin, 1985*). The split S waves are called S1 and S2 waves and propagate with different velocities and have different polarizations. Observations of S-wave splitting have been reported in the Earth's crust for decades (*Babuška and Cara, 1991*; *Savage, 1999*). They indicate the presence of preferably oriented structures in the crust such as layers, parallel aligned fractures, cracks, micro-cracks (*Crampin, 1981*; *Nishizawa, 1982*; *Peacock and Hudson, 1990*) or the presence of minerals with a preferred orientation in rocks. Studying anisotropy helps in understanding the stress history, deformation and faulting of the crust.

Crustal anisotropy in the West Bohemia/Vogtland region and in adjacent areas has been studied by many authors. In adjacent areas, anisotropy was detected using active refraction experiments, performed in the Bohemian Massif (*Růžek et al., 2003*; *Vavryčuk et al., 2004*) and using numerous seismic experiments performed at the KTB site (*Rabbel, 1994*; *Jahns et al., 1996*; *Rabbel and Mooney, 1996*; *Berckhemer et al., 1997*; *Rabbel et al., 2004*; *Okaya et al., 2004*), which is about 50 km SW from the target area. In the target area, anisotropy was detected using laboratory measurements of the P-wave velocity on rock samples (*Pros et al., 1998*; *Martínková et al., 2000*; *Chlupáčová et al., 2003*), using P-wave travel times measured for micro-earthquakes and quarry blasts (*Málek et al., 2005*), and using the S-wave splitting observations in records of micro-earthquakes that occurred during the 1985/86 earthquake swarm (*Vavryčuk, 1993, 1995*). The studies show that the orientation of anisotropy is generally consistent over the whole area. The azimuth of the polarization direction of the fast S wave ranges usually from 115° to 135° NE and roughly coincides with the orientation of the maximum compression in the region, characterized by azimuths between 145−160° (*Havíř, 2000*; *Wirth et al., 2000*; *Vavryčuk, 2002*). The tectonic stress field in the West Bohemia region is similar to that in the other parts of the Bohemian Massif (*Peška, 1992*), in its adjacent areas as in the KTB (*Brudy et al., 1997*, azimuth 160°±10°), and in Central Europe (*Müller et al., 1992*, azimuth 144°±26°). The overall S-wave anisotropy in the West Bohemia area, estimated from S-wave splitting, is about 6% (*Vavryčuk, 1993*). However, laboratory measurements indicate that a detail anisotropy pattern might be more complicated. The symmetry and strength of anisotropy is likely to vary being different for different rocks in the area (granites, phyllites, gneisses, mica schists, amphibolites).

The aim of this paper is to utilize an extensive dataset of records of local micro-earthquakes in the West Bohemia/Vogtland region, gathered in the period of 1991 to 2007, in order to carry out a detailed S-wave splitting analysis. The work should expand and refine the results obtained by *Vavryčuk (1993, 1995)* by providing more accurate and more comprehensive knowledge of the anisotropy in the area.

2. SEISMIC ACTIVITY IN THE WEST BOHEMIA/VOGTLAND REGION

The West Bohemia/Vogtland region is the most seismically active region in the Bohemian Massif, which is the largest stable outcrop of Variscan rocks in Central Europe. The western part of the Bohemian Massif represents a junction of three tectonic units (*Franke, 2000*; *Babuška et al., 2007*; *Babuška and Plomerová, 2008*): Saxothuringian, Teplá-Barrandian and Moldanubian. The boundaries between the units are formed by the Tertiary Eger Rift, a 300 km long ENE-WSW striking structure characterized by high heat flow, and by the West Bohemia Shear-Zone, striking NWN-SES. Active tectonics are manifested by numerous mineral springs, emanations of CO_2, presence of Tertiary to

Quaternary volcanism, neotectonic crustal movements, and by persistent seismic activity with frequent occurrence of earthquake swarms.

In the West Bohemian part of the seismically active area, earthquake activity is monitored by the WEBNET (*Horálek et al., 2000*) and KRASNET (*Nehybka and Skácelová, 1995*) local networks, which are formed by 10 and 5 three-component digital seismic stations equipped with short-period seismometers and connected to a data centre by telemetry. The magnitude threshold of the networks is about –0.5. The epicentres of micro-earthquakes are scattered over an area of about 50×70 km. The depth of hypocentres ranges from 2 to 23 km. The most prominent recent periods of seismic activity were earthquake swarms in 1985/86, 1989/90, 1994, 1997 and in 2000, which comprised hundreds to thousands of micro-earthquakes (*Vavryčuk, 1993*; *Fischer and Horálek, 2000, 2003*; *Horálek et al., 2000*). The strongest earthquake in the last 40 years was the earthquake of magnitude 4.6 which occurred on December 23, 1985 in the Nový Kostel focal area. The Nový Kostel focal area is characterized by the most intense seismic activity in the region.

3. S-WAVE SPLITTING OBSERVATIONS

3.1. Data

Studying crustal anisotropy by means of S-wave splitting is a data demanding analysis, which can be carried out only under the following conditions. First, the ray coverage of the focal sphere should be good enough to measure directional variations of the S-wave splitting. Measuring the directional variations is essential for determining the orientation, symmetry and strength of anisotropy. Second, the data should ensure that rays sample densely the whole region under study. This is important for detecting anisotropy inhomogeneities if present. Both conditions seem to be satisfied by the seismicity in the West Bohemia/Vogtland region, where a huge number of shallow micro-earthquakes covers the epicentral region with foci at different depths and has been monitored by relatively dense seismic networks (see Fig. 1).

We have processed seismic data from the period 1991–2007, recorded at the stations of the WEBNET network. The SeisBase code was used as the basic tool for visualizing and analyzing the data (*Fischer and Hampl, 1997*). The seismic records were pre-processed by frequency filtering. High-frequency reverberations, which complicate particle motions (see *Vavryčuk, 1993, Fig. 4a*), were removed by a 40 Hz low-pass filter. We analyzed the velocity records for zero or low delay times between split S waves. For sufficiently high delay times, we integrated the velocity records to obtain displacement records, which we filtered with a 2 Hz high-pass filter to remove the static offset and linear trend. This procedure usually enhanced the clarity of seismograms and particle motions (see *Vavryčuk, 1993, Fig. 4b*), and helped with the identification of split S waves (compare Figs. 2 and 3). The S-wave particle motions were plotted in horizontal projection and the prevailing polarization directions of the S1 and S2 waves were estimated by visual inspection.

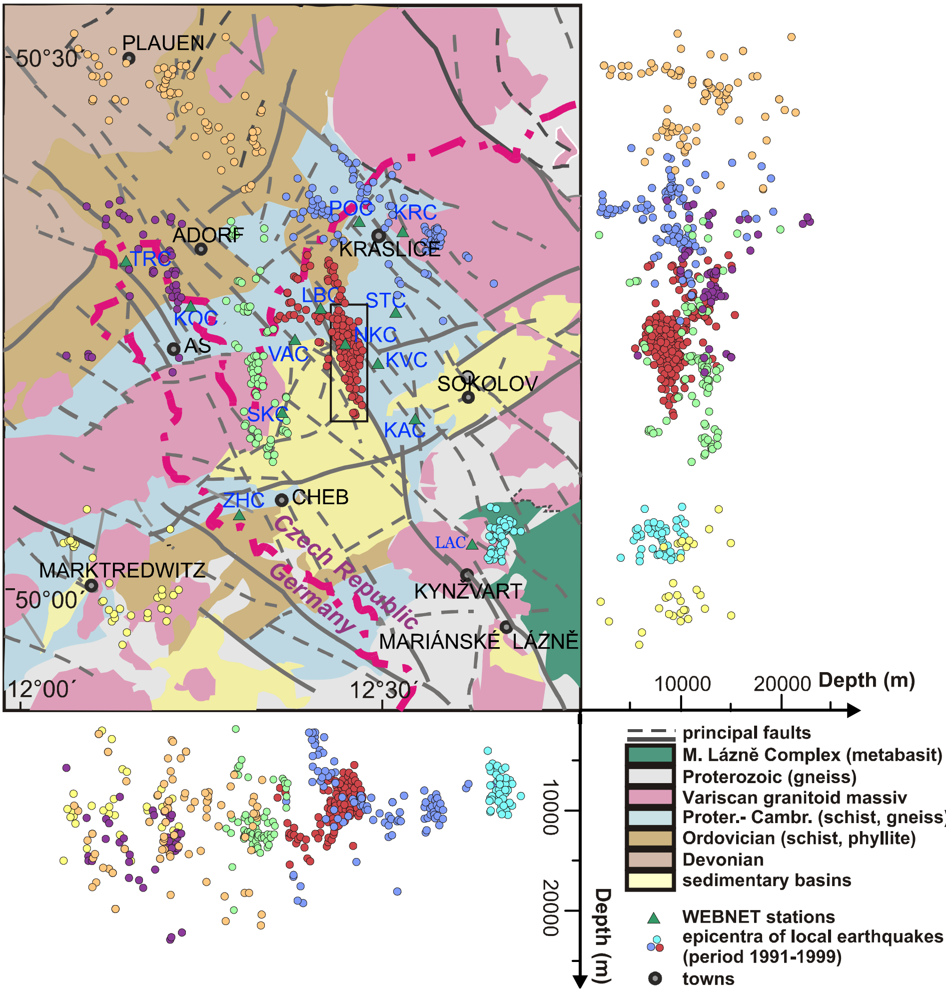

Fig. 1. Map of the West Bohemia/Vogtland seismically active area. The WEBNET stations are marked by green triangles, the epicentres of micro-earthquakes are marked by colour-coded dots in order to distinguish different seismically active zones. The seismic activity is shown for the period of 1991–1999. The Nový Kostel seismically active zone is marked by the rectangle.

3.2. Foci from the Nový Kostel Area

First, we analyzed the S-wave splitting observations in the records of events which occurred in the Nový Kostel focal area. Since the focal area is very small with respect to the aperture of the seismic network, we can assume that all rays connecting the foci with the stations form effectively a bundle of rays with one common point at the source. The rays are assumed to be straight lines. This should roughly estimate the average direction of a ray, which is actually a curve due to a velocity gradient. Since the focal area lies

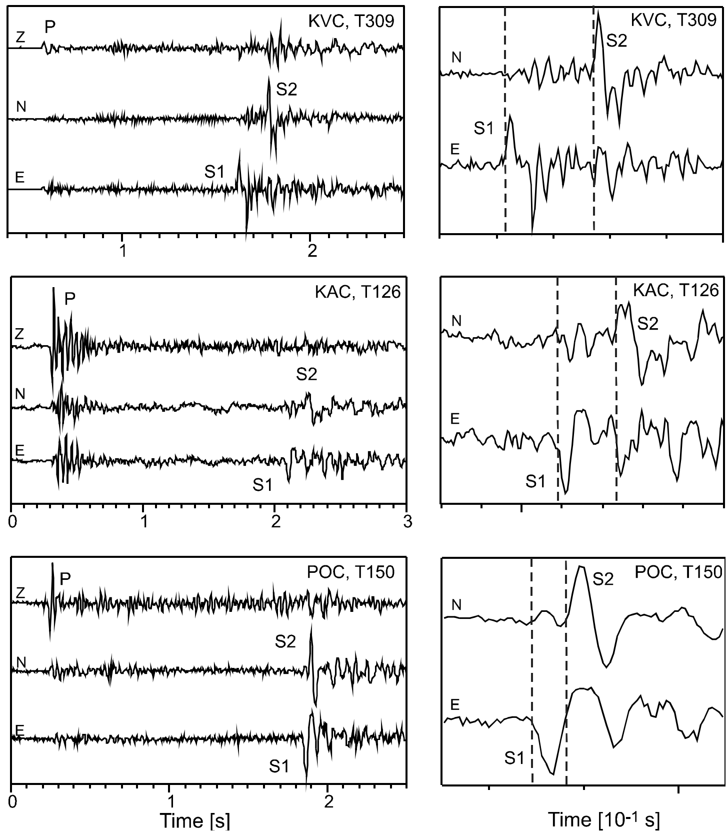

Fig. 2. Examples of velocity records of three events recorded at three different stations. Left-hand plots - three-component records of P and S waves, right-hand plots - a detail of the horizontal S-wave traces. The *z*-axis in the left-hand plots is directed upward. The vertical dashed lines mark the arrivals of the split S waves. For event identifications, see Table 1.

inside the network, the ray coverage of the focal sphere is very good. To analyse a sufficiently large dataset, we included all the data available with no restriction to the so-called shear-wave window. The waveforms outside the shear-wave window are expected to be distorted, because of the complex interaction of waves with the surface. However, based on our experience, we observed no essential differences between the particle motions inside or outside this window, and we met no significant problems with interpreting the particle motions associated with shallow rays. The expected complications probably do not occur so often because of the presence of low-velocity subsurface layers which are responsible for the majority of rays arriving sufficiently steeply at the surface.

Fig. 4 shows 229 ray directions of 70 analyzed events together with some examples of a distinct S-wave splitting observed at various stations. Information on events used as examples is summarized in Table 1. The vast majority of the analyzed particle motions

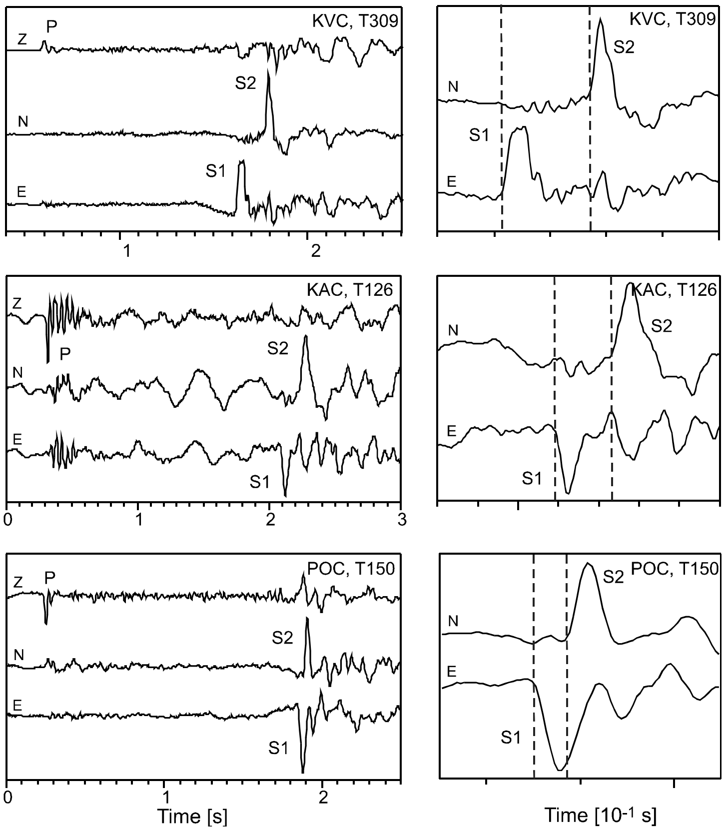

Fig 3. Examples of displacement records of three events recorded at three different stations. The events and the stations are the same as in Fig. 2. Left-hand plots - three-component records of P and S waves, right-hand plots - a detail of the horizontal S-wave traces. The *z*-axis in the left-hand plots is directed upward. The vertical dashed lines mark the arrivals of the split S waves. For event identifications, see Table 1.

display S-wave splitting with approximately perpendicular directions of the fast and slow split waves. For some events, the fast and slow waves are well separated and their polarization is almost linear. However, such observations are rather rare. The separated split waves are frequently observed to have not a linear but elliptical, or even more complicated polarization. Fig. 4 also shows that the polarization directions of split S waves are roughly consistent over the whole area. The fast wave is predominantly aligned NW-SE being close to the direction of the maximum compression in the area (referred to as “normal splitting”). For some rays, the fast wave is aligned NE-SW rather being perpendicular to the maximum compression (“reverse splitting”). The directions of the reverse splitting observations are less frequent in Fig. 4 and seem to be rather isolated and randomly scattered over the focal sphere.

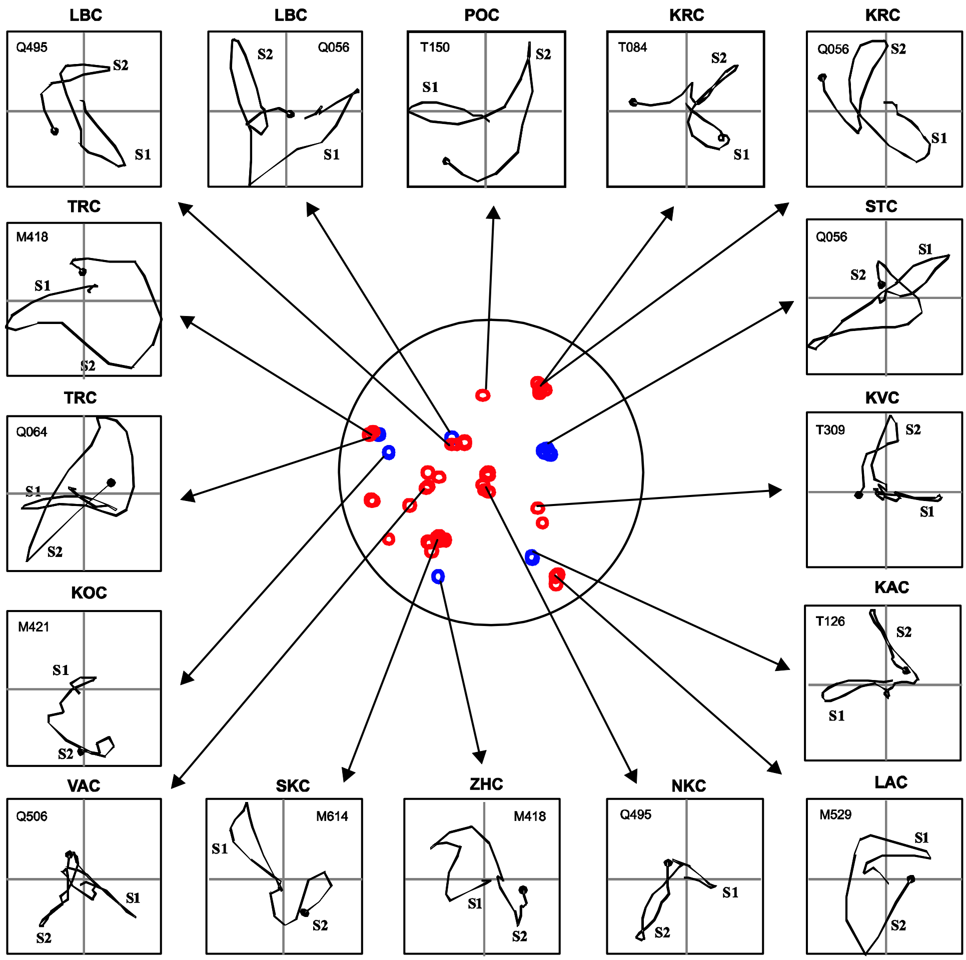

Fig. 4. Observations of S-wave splitting in records of the WEBNET stations. The foci of 70 micro-earthquakes from the period of 1991–2007 are located in the Nový Kostel seismically active area. Circles on the focal sphere show directions of rays from source to station. The red/blue colour indicates normal/reverse splitting. Particle motions are shown in the horizontal projection. The endpoint in the particle motion is denoted by the dot. Upper hemisphere equal-area projection is used. For the identification of the events shown at the particle motions, see Table 1.

3.3. Irregularities in the S-Wave Polarizations

Not all particle motions display a distinct S-wave splitting with the fast and slow waves polarized parallel or perpendicular to the NW-SE direction (Fig. 4). Exceptionally, the mutually perpendicular split S waves have polarizations which can deviate from the commonly observed polarization directions (see Table 2). This is observed, for example, for the events with foci at the Nový Kostel area recorded at the KVC station (see Figs. 5a

Table 1. Events with distinct S-wave splitting at the WEBNET stations. ID is the identification code of an event in the WEBNET database, OT is the origin time of the event, STA denotes the station, Z the depth, R the hypocentral distance, and M_L the local magnitude.

ID	Date	OT	STA	E [°]	N [°]	Z [km]	R [km]	M_L
M418	17.1.1997	22:57:38	TRC	12.442	50.236	8.99	24.4	3.0
M418	17.1.1997	22:57:38	ZHC	12.442	50.236	8.99	22.8	3.0
M421	17.1.1997	23:04:35	KOC	12.446	50.238	9.17	18.2	1.2
M529	18.1.1997	06:38:29	LAC	12.442	50.237	8.95	26.4	1.2
M614	18.1.1997	13:33:40	SKC	12.445	50.237	8.77	13.3	1.0
Q056	17.1.2001	02:27:51	KRC	12.456	50.240	7.07	13.9	1.8
Q056	17.1.2001	02:27:51	LBC	12.456	50.240	7.07	8.8	1.8
Q056	17.1.2001	02:27:51	STC	12.456	50.240	7.07	9.2	1.8
Q064	17.1.2001	02:46:08	TRC	12.455	50.240	6.78	24.3	0.7
Q495	12.7.2001	21:44:49	NKC	12.450	50.245	7.17	7.8	0.5
Q495	12.7.2001	21:44:49	LBC	12.450	50.245	7.17	8.6	0.5
Q506	13.7.2001	13:26:11	VAC	12.451	50.245	7.16	9.4	0.4
T084	28.2.2004	02:30:57	KRC	12.453	50.246	6.97	13.4	0.8
T126	11.3.2004	07:27:03	KAC	12.447	50.240	8.93	15.1	0.4
T150	9.4.2004	11:38:27	POC	12.448	50.238	8.98	13.3	0.4
T309	30.12.2004	04:00:58	KVC	12.454	50.218	7.49	9.3	0.4

and 6a): the S1 wave is polarized in the E-W direction and the S2 wave in the N-S direction. Sometimes it also happens that the S waves are distinctly split but in directions no longer mutually perpendicular (see Fig. 6b). Finally, no or negligible S-wave splitting or an anomalous and complex S-wave polarization is observed for some events (see Fig. 6c). This happens, when direct S waves interfere with scattered waves, generated by inhomogeneities in the medium, or when the delay time between split S waves is not sufficiently large for separating the S1 and S2 waves. All the above-mentioned irregularities and anomalies in the S-wave polarizations are rather rare.

3.4. Foci from the Whole Seismically Active Area

A quite different pattern of S-wave splitting observations is obtained in studying events located in various focal areas and recorded at one particular station (see Fig. 7). For example, only normal splitting with a few exceptions of no splitting is observed at the NKC station. At station VAC, normal as well as reverse splitting is observed, but normal splitting prevails. Interestingly, the spatial distribution of reverse splitting is not random as in Fig. 4, but forms a well-defined cluster. On the contrary, reverse splitting is predominantly observed at the STC station. The rays with normal splitting are well clustered. A similar pattern as in Fig. 4 is observed at the LBC station. The predominant type is normal splitting, and the directions with the reverse splitting observations are isolated and scattered over the whole focal sphere.

More detailed information on the orientation and strength of anisotropy can be obtained from measurements of delay times between split S waves. Fig. 8 shows the directional variation of the delay times measured at stations VAC, NKC, STC and LBC.

The delay times are normalized to hypocentral distance of 1 km. Since the delay times were significantly scattered, they had to be smoothed. The large scatter probably originated in errors when picking the slow S wave. The slow S wave was frequently lost in scattered waves, so that its identification was difficult and its arrival time was measured with low accuracy. In interpreting Fig. 8, we also have to keep in mind that the delay times represent an overall quantity accumulated along the whole ray path. This may make the interpretation of delay times difficult if the anisotropy is spatially dependent. For spatially dependent anisotropy, the contributions from different ray path segments overlap and their separation is either extremely difficult or impossible.

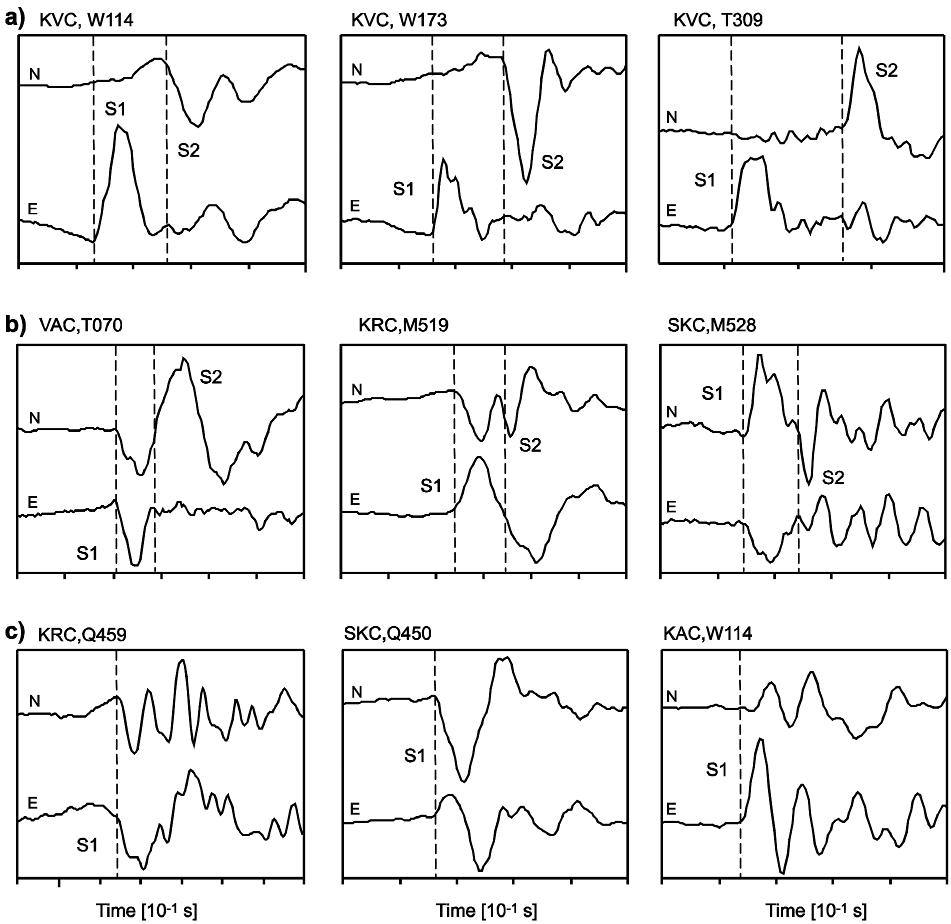

Fig. 5. Displacement records of S waves with irregular splitting or with anomalous polarizations. **(a)** S-wave splitting with rotated directions of the fast and slow S waves, **(b)** split S waves with non-orthogonal polarization directions, **(c)** anomalous S-wave particle motions. The vertical dashed lines mark the arrival time. Only the arrival of the fast S wave is marked in plots (c) because the slow S wave could not be reliably identified. For event identifications, see Table 2.

Fig. 8 shows that the delay times at all analyzed stations display one global minimum and one global maximum in directions which are approximately perpendicular. This indicates a simple type of anisotropy for which the maximum and minimum delay times correspond to the directions of the anisotropy axes. Obviously, for more complicated delay time variations, this simple relation is no longer valid. At all analyzed stations, the symmetry axes inferred from the delay time patterns are inclined. The inclination of the symmetry axes varies with the position of the station. The symmetry axes of anisotropy are inclined even for the NKC station, which displays a rather uniform normal splitting pattern in Fig. 7. The delay time measurements in Fig. 8 reveal that the order of the split S waves is uniform at the NKC station, but the delay times are not uniform and display a systematic spatial variation.

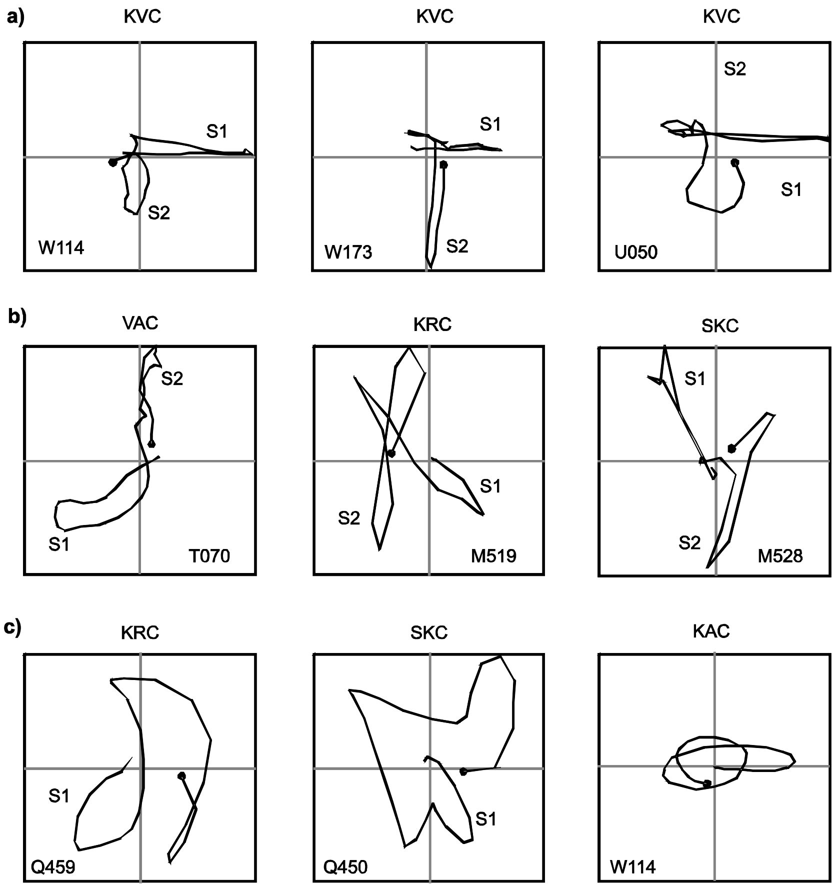

Fig. 6. Particle motions of S waves with irregular splitting or with anomalous polarizations. **(a)** S-wave splitting with rotated directions of the fast and slow S waves, **(b)** split S waves with non-orthogonal polarization directions, **(c)** anomalous S-wave particle motions. The endpoint of the particle motion is marked by the dot. The particle motions are shown in horizontal projection. For the event identifications, see Table 2.

Table 2. Events with irregular S-wave splitting or with anomalous polarization. For the meaning of the quantities, see the caption of Table 1.

ID	Date	OT	STA	E [°]	N [°]	*Z* [km]	*R* [km]	M_L
M519	18.1.1997	05:34:15	KRC	12.442	50.237	9.05	15.7	2.3
M528	18.1.1997	06:28:08	SKC	12.442	50.237	8.94	13.3	1.2
Q450	13.6.2001	18:21:44	SKC	12.449	50.212	9.54	12.7	1.5
Q459	14.6.2001	09:27:40	KRC	12.449	50.213	9.58	17.7	0.8
T070	22.2.2004	16:46:39	VAC	12.427	50.214	13.34	14.5	0.9
U050	16.3.2005	09:51:00	KVC	12.437	50.222	9.63	11.7	0.5
W114	9.2.2007	13:53:12	KAC	12.453	50.201	9.45	11.0	1.5
W114	9.2.2007	13:53:12	KVC	12.453	50.201	9.45	12.7	1.5
W173	9.2.2007	15:21:48	KVC	12.455	50.202	9.34	10.9	1.0

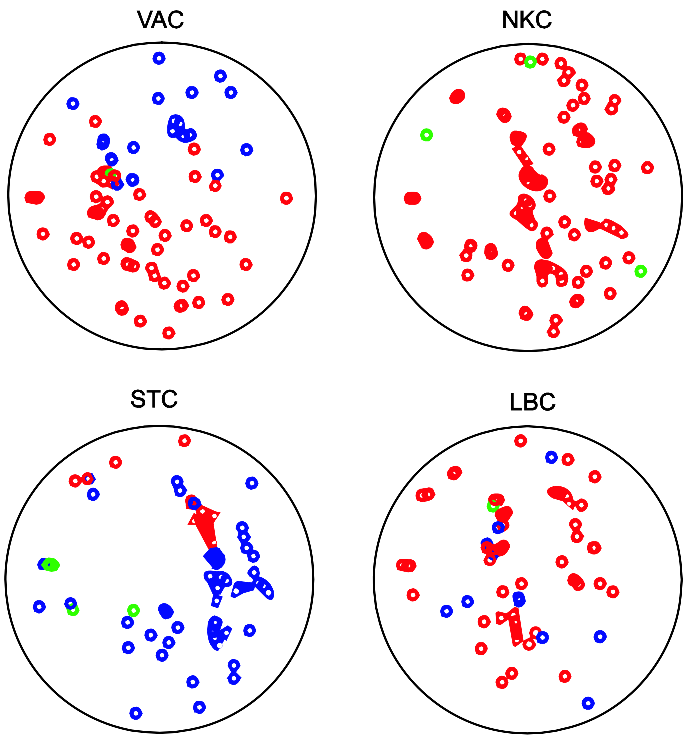

Fig. 7. Observations of S-wave splitting in records of stations VAC (117 events), NKC (129 events), STC (139 events) and LBC (86 events). The foci of the micro-earthquakes are scattered over the whole seismically active area of the West Bohemia/Vogtland region. Circles in the focal sphere show directions of rays from source to station. The red/blue/green colour indicates normal/reverse/no splitting. Upper hemisphere equal-area projection is used.

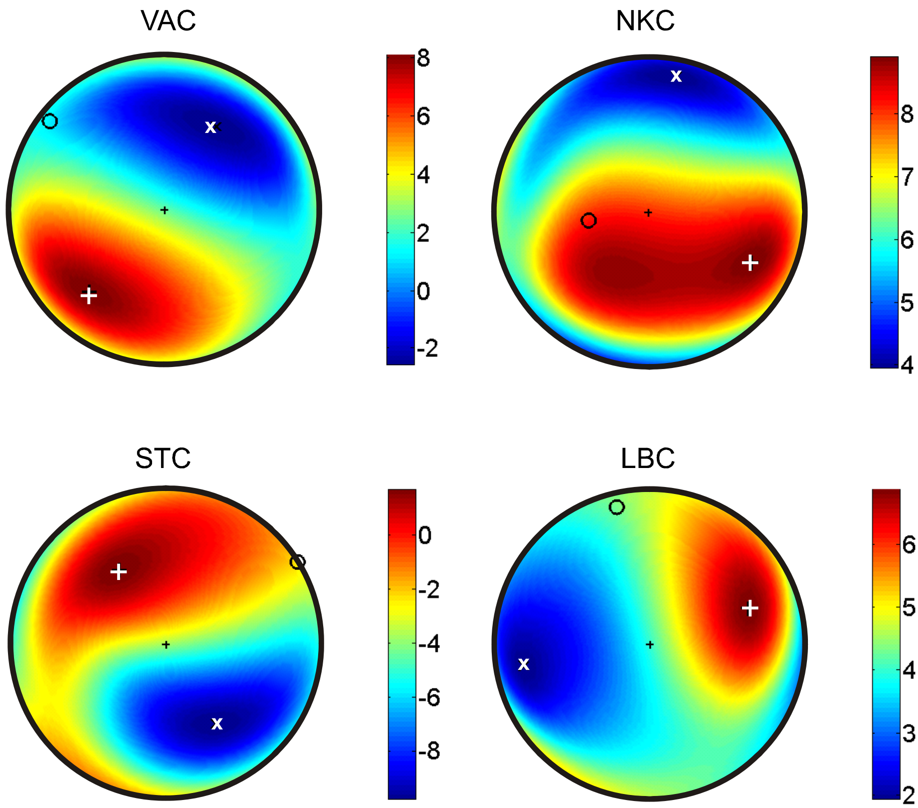

Fig. 8. Delay-time observations of split S waves in records of stations VAC, NKC, STC and LBC. The delay times are normalized to 1 km of the ray path and measured in microseconds. The measurements are performed for the points shown in Fig. 7 and further averaged to obtain a smooth spatial variation. The symbols '**+**' and '**×**' mark the directions with the maximum and minimum delay times, respectively. The symbol '**O**' marks the direction perpendicular to the maximum and minimum delay time directions. Note that the red/blue colour does not necessarily correspond to normal/reverse splitting. The normal/reverse splitting is characterized by the positive/negative values of the delay times. Upper hemisphere equal-area projection is used.

3.5. Effects of Focal Mechanisms on S-Wave Splitting

Although the polarization directions of split S waves are rather stable at each station, the particle motions may display some variations. A detailed analysis reveals that the S-wave splitting may vary even for waves recorded at the same station and propagating along the same ray direction. Fig. 9 shows the S-wave particle motions of 9 events, which occurred at the Nový Kostel focal area and were recorded at the NKC station. The station lies exactly above the focal area. Since the foci are very close to each other (within an epicentral area of 600 × 900 m), the rays have effectively the same direction, which is almost vertical (see Table 3). All events display clear splitting of the normal type with similar polarization directions of the fast and slow waves. However, as visible in the particle motion diagrams, the polarity of split S waves and their amplitude ratio varies. Consequently, the original isotropic S wave reconstructed from both the split waves has a variable direction.

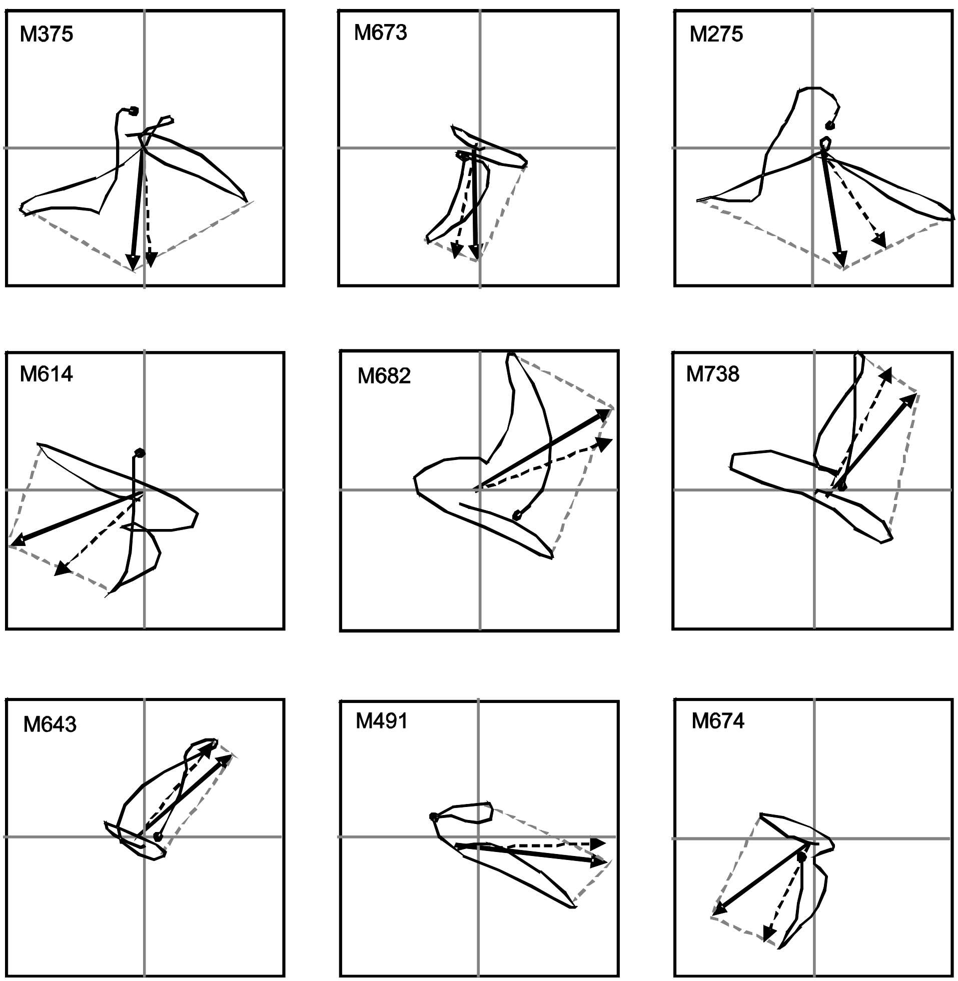

Fig. 9. Effects of the focal mechanisms on split S waves. Horizontal particle motions of split S waves are shown for 9 micro-earthquakes that occurred in the Nový Kostel seismically active area and were recorded at the NKC station (see Table 3). The full arrows show the directions of the S wave reconstructed from split S waves. The dashed arrows show the directions of the isotropic S waves predicted from the focal mechanisms (see Table 4).

The observation of different polarities and amplitudes of split S waves may indicate a variety of focal mechanisms (see *Kaneshima et al., 1990*). To confirm this idea, Fig. 9 shows the comparison of the polarization direction of the S wave obtained as the vector sum of the split S waves and that predicted from the focal mechanism (see Table 4). Even though the determination of the polarization direction of the S wave, reconstructed from the particle motions of split S waves, was very rough, the directions of the reconstructed and calculated S waves are generally consistent. Some inconsistencies observed probably arise from the inaccuracy of the focal mechanisms, because they were inverted using an isotropic Green's function. Hence, exploiting the "isotropic" S wave, reconstructed from split anisotropic S waves, could, in principle, improve the accuracy of the focal mechanism inversion.

Table 3. Events with varying S-wave splitting at the NKC station. *A* and *I* denote the geometrical ray azimuth measured clockwise from the North and the geometrical ray incidence measured from the vertical direction. For the meaning of other quantities, see the caption of Table 1.

ID	Date	OT	E [°]	N [°]	*Z* [km]	M_L	*A* [°]	*I* [°]
M275	16.1.1997	15:11:20	12.447	50.235	9.12	1.9	187	2.1
M375	17.1.1997	07:48:09	12.451	50.236	9.23	1.0	190	2.5
M491	18.1.1997	02:16:39	12.449	50.235	9.19	0.7	202	2.2
M614	18.1.1997	13:33:41	12.444	50.236	8.82	1.0	159	3.0
M643	18.1.1997	21:28:28	12.444	50.237	8.78	0.8	167	3.6
M673	19.1.1997	08:48:57	12.442	50.235	8.23	0.4	148	4.0
M674	19.1.1997	08:49:43	12.442	50.236	8.40	0.7	144	4.0
M682	19.1.1997	14:57:14	12.447	50.239	9.34	0.7	179	4.6
M738	21.1.1997	21:50:21	12.445	50.237	9.19	0.4	167	3.1

Table 4. Focal mechanisms of events with varying S-wave splitting at the NKC station. ISO, DC and CLVD denote the isotropic, double-couple and compensated linear vector dipole components. Their percentages have been calculated using Eqs.(14)–(17) of *Vavryčuk (2005)*.

ID	Date	OT	Strike [°]	Dip [°]	Rake [°]	ISO [%]	DC [%]	CLVD [%]
M275	16.1.1997	15:11:20	216	78	–30	–9.5	71.6	–18.9
M375	17.1.1997	07:48:09	191	49	–52	–13.6	82.2	–4.2
M491	18.1.1997	02:16:39	32	66	47	10.1	82.6	7.3
M614	18.1.1997	13:33:41	226	46	–16	–14.7	59.0	–26.4
M643	18.1.1997	21:28:28	275	79	166	12.3	79.1	8.5
M673	19.1.1997	08:48:57	219	55	–35	–11.4	59.4	–29.2
M674	19.1.1997	08:49:43	221	52	–28	–10.4	62.9	–26.7
M682	19.1.1997	14:57:14	35	54	48	19.7	41.1	39.1
M738	21.1.1997	21:50:21	259	67	145	13.0	86.8	0.3

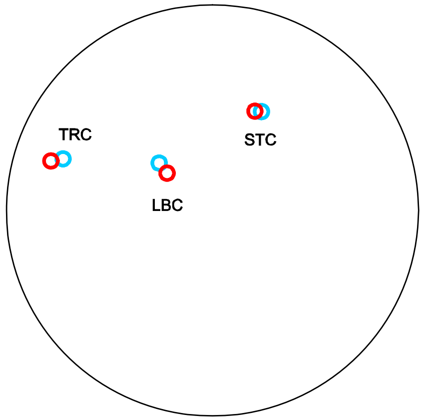

Fig. 10. Three pairs of rays with the 90°-flip observations projected onto the focal sphere. Upper hemisphere equal-area projection is used. The red/blue colour corresponds to normal/reverse splitting.

3.6. Observations of 90°-Flips of S Waves

Figs. 4 and 7 show that the areas on the focal sphere, characterized by the normal or reverse splitting, are not always well separated, but they can touch or even overlap in some exceptional cases. Hence, in some directions it is possible to observe a different type of splitting for different events. Fig. 10 shows a focal sphere with three pairs of rays. The rays in each pair have almost identical directions, but the splitting types are opposite (see Fig. 11, Table 5). The permutation of arrivals of the split S waves for the same ray direction is referred to as "90º-flips of S waves" and is usually attributed to temporal variations of anisotropy (*Crampin et al., 2004*).

4. DISCUSSION

The S-wave splitting observations in records of micro-earthquakes that occurred in the period of 1991–2007 indicate that the anisotropy pattern in the West Bohemia/Vogtland region is more complex than indicated by previous studies. Based on observations of events from the Nový Kostel focal area recorded at a few stations, *Vavryčuk (1993, 1995)* proposed a transversely isotropic model of the crust with a horizontal symmetry axis. The azimuth of the symmetry axis was 31°NE and roughly perpendicular to the maximum compression in the region. All observations displayed normal splitting; *Vavryčuk (1993, 1995)* detected no reverse splitting. In this study, a far more extensive dataset is analysed and reveals that normal as well as reverse splitting can occur in the region. The anisotropy pattern appears to depend strongly on the position of the seismic station (Fig. 7). Surprisingly, at some stations, reverse splitting is detected not only in isolated ray directions, but in the majority of directions being thus the prevailing type of splitting observed at a particular station. The pattern of the normal/reverse splitting on a focal sphere for some stations suggests that the symmetry axes of anisotropy might be inclined.

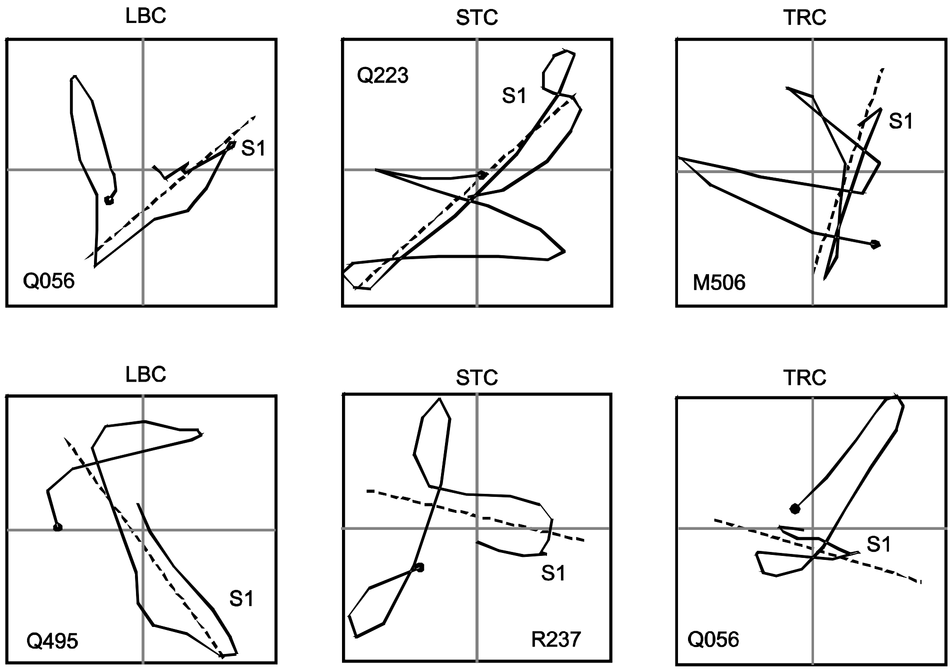

Fig. 11. Velocity particle motions for three pairs of events with similar ray directions but of opposite types of splitting. For information about the events, see Table 5.

Bokelmann (1995) proposed an inclined anisotropy in the West Bohemia/Vogtland region, but the limited amount of data available at that time was not sufficient to provide clear evidence for this statement. The inclined anisotropy axes are now supported by the normal/reverse splitting patterns at the VAC and STC stations, which are distinctly asymmetric with respect to the vertical axis (Fig. 7). The normal/reverse splitting pattern at the NKC and LBC stations is nearly uniform and provides no indication of an inclined anisotropy. However, inclined anisotropy is in evidence at all analyzed stations when measuring the delay times between the split S waves (Fig. 8). If we identify the symmetry axes with the directions of the maximum and minimum values of delay times normalized to 1 km of the ray path, the anisotropy under all analyzed stations appears inclined. The delay times display values of up to almost 10 ms per 1 km of the ray path. These values correspond roughly to an S-wave anisotropy strength of 3.5% provided the anisotropy is homogeneous along the whole ray path. If we assume that the anisotropic structure is located in the topmost part of the Earth's crust, down to 3−4 km beneath a station, the estimated strength of anisotropy then increases to about 7−15%.

Note that inclined anisotropic structures in the upper Earth's crust are observed and documented also in adjacent areas as, for example, at the KTB site in Germany (*Okaya et al., 2004*; *Rabbel et al., 2004*). The presence of inclined anisotropic structures is indicated also in the subcrustal lithosphere in the western part of the Bohemian Massif inferred from

Table 5. Events displaying the 90°-flips of the split S waves. Type denotes normal (N) or reverse (R) S-wave splitting. *A* and *I* denote the geometrical ray azimuth measured clockwise from the North and the geometrical ray incidence measured from the vertical direction, *R* is the hypocentral distance, M_L is the local magnitude, and *Dt* is the delay time between split S waves.

ID	Date	OT	STA	E [°]	N [°]	*Z* [km]	*R* [km]	M_L	Type	*A* [°]	*I* [°]	*Dt*[ms]
M506	18.1.1997	04:24:57	TRC	12.444	50.236	8.96	24.5	0.5	R	161	67	–24
Q056	17.1.2001	02:27:51	TRC	12.456	50.240	7.07	24.5	1.8	N	163	72	68
Q056	17.1.2001	02:27:51	LBC	12.456	50.240	7.07	8.8	1.8	R	138	29	–56
Q495	12.7.2001	21:44:49	LBC	12.450	50.245	7.17	8.6	0.5	N	140	25	52
Q223	23.5.2001	21:56:45	STC	12.461	50.179	9.23	14.9	0.5	R	65	45	–72
R237	7.12.2002	03:23:48	STC	12.467	50.180	9.22	13.8	0.2	N	67	44	52

splitting of S- and SKS-waves of regional and teleseismic earthquakes (*Plomerová et al., 2007*; *Babuška et al., 2008*).

Strongly dependent normal/reverse splitting patterns and delay-time patterns on a station position point to non-uniform anisotropy in the region. This would indicate that anisotropy is not primarily a stress related phenomenon (e.g., anisotropy due to the presence of stress aligned cracks in rocks), because the stress field seems to be rather homogeneous over the whole area. Anisotropy is more likely related to or affected by the intrinsic rock structure and alignment of minerals in rocks. The spatial variation of anisotropy thus probably reflects the presence of a variety of different types of anisotropic rocks in the region. A diverse geological pattern in the region with the presence of granites, amphibolites, mica schists and gneisses is reported, for example, by *Chlupáčová et al. (2003, Fig. 1)* who also mention a high variation of anisotropy strength for individual rocks measured on selected rock samples in the laboratory.

A very intriguing phenomenon is the observation of the 90°-flips of the split S waves, i.e., the observation of normal as well as reverse splitting in one fixed ray direction, or in two directions which are very close to one another. So far, we have detected several 90°-flips, but only in isolated and rather rare cases (see Figs. 10 and 11). A more detailed and thorough analysis is needed to decide whether the observed flips are the result of a temporal variation of anisotropy or not. Since the seismic activity in the West Bohemia/Vogtland region is probably triggered or driven by crustal fluids (*Vavryčuk, 2002*; *Horálek and Fischer, 2008*), the 90°-flips of the split S waves would become an attractive tool for monitoring fluid migration and long-term fluid flow.

Acknowledgements: We thank V. Babuška, T. Plenefisch and an anonymous reviewer for their helpful reviews. The work was supported by the Grant Agency of the Academy of Sciences of the Czech Republic, Grant No. IAA300120801, and the Grant Agency of the Czech Republic, Grant No. 205/06/1780.

References

Babuška V. and Cara M., 1991. *Seismic Anisotropy in the Earth*. Kluwer Academic Publ., Dordrecht, The Netherlands.

Babuška V. and Plomerová J, 2008. Control of paths of Quaternary volcanic products in western Bohemian Massif by rejuvenated Variscan triple junction of ancient microplates. *Stud. Geophys. Geod.*, **52**, 607–629.

Babuška V., Plomerová J. and Fischer T., 2007. Intraplate seismicity in the western Bohemian Massif (central Europe): A possible correlation with a paleoplate junction. *J. Geodyn.*, **44**, 149–159.

Babuška V., Plomerová J. and Vecsey L., 2008. Mantle fabric of western Bohemian Massif (central Europe) constrained by 3D seismic P and S anisotropy. *Tectonophysics*, doi: 10.1016/j.tecto.2008.01.020 (in print).

Berckhemer H., Rauen A., Winter H., Kern H., Kontny A., Lienert M., Nover G., Pohl J., Popp T., Schult A., Zinke J. and Soffel H.C., 1997. Petrophysical properties of the 9-km-deep crustal section at KTB. *J. Geophys. Res.*, **102(B8)**, 18337–18361.

Bokelmann G.H.R., 1995. Comment on "Crustal anisotropy from local observations of shear-wave splitting in West Bohemia, Czech Republic," by V. Vavryčuk. *Bull. Seismol. Soc. Amer.*, **85**, 653–657.

Brudy M., Zoback M.D., Fuchs K., Rummel F. and Baumgärtner J., 1997. Estimation of the complete stress tensor to 8 km depth in the KTB scientific drill holes: Implications for crustal strength. *J. Geophys. Res*., **102(B8)**, 18453–18475.

Chlupáčová M., Skácelová Z. and Nehybka V., 2003. P-wave anisotropy from the seismic area in Western Bohemia. *J. Geodyn.*, **35**, 45–57.

Crampin S., 1981. A review of wave motion in anisotropic and cracked elastic media. *Wave Motion*, **3**, 343–391.

Crampin S., 1985. Evaluation of anisotropy by shear-wave splitting. *Geophysics*, **50**, 142–152.

Crampin S., Peacock S., Gao Y. and Chastin S., 2004. The scatter of time-delays in shear-wave splitting above small earthquakes. *Geophys. J. Int.*, **156**, 39–44.

Fischer T. and Hampl F., 1997. SeisBase - principles of a program and database for routine analysis of data from local seismic networks. *Acta Montana A*, **11**, 15–34.

Fischer T. and Horálek J., 2000: Refined locations of the swarm earthquakes in the Nový Kostel focal zone and spatial distribution of the January 1997 swarm in Western Bohemia, Czech Republic. *Stud. Geophys. Geod.*, **44**, 210–226.

Fischer T. and Horálek J., 2003: Space-time distribution of earthquakes swarms in the principal focal zone of the NW Bohemia/Vogtland seismoactive region: period 1985–2001. *J. Geodyn.*, **35**, 125–144.

Franke W., 2000. The mid-European segment of the Variscides: tectonostratigraphic units, terrane boundaries and plate tectonic evolution. In: Franke W., Haak V., Oncken O. and Tanner D. (Eds.), *Orogenic Processes: Quantification and Modelling in the Variscan Belt*. *Geol. Soc. Spec. Publ. London*, **179**, 35–61.

Havíř J., 2000. Stress analyses in the epicentral area of Nový Kostel (Western Bohemia). *Stud. Geophys. Geod.*, **44**, 522–536.

Horálek J., Fischer T., Boušková A. and Jedlička P., 2000. The Western Bohemia/Vogtland region in the light of the WEBNET network. *Stud. Geophys. Geod.*, **44**, 107−125.

Horálek J. and Fischer T., 2008. Crustal fluids in triggering the West Bohemia/Vogtland earthquake swarms: just what we know (a review). *Stud. Geophys. Geod.*, **52**, 455–478.

Jahns E., Rabbel W. and Siegesmund S., 1996. Quantified seismic anisotropy at different scales: a case study from the KTB crustal segment. *J. Geol. Wiss.*, **24**, 729–740.

Kaneshima S., Maeda N. and Ando M., 1990. Evidence for the splitting of shear waves from waveforms and focal mechanism analyses. *Phys. Earth Planet. Inter.*, **61**, 238–252.

Málek J., Horálek J. and Janský J., 2005. One-dimensional qP-wave velocity model of the upper crust for the West Bohemia/Vogtland earthquake swarm region. *Stud. Geophys. Geod.*, **49**, 709−730.

Martínková M., Pros Z., Klíma K., Lokajíček T. and Kotková J., 2000. Experimentally determined P-wave velocity anisotropy for rocks related to the Western Bohemia seismoactive region. *Stud. Geophys. Geod.*, **44**, 581−589.

Müller B., Zoback M.L., Fuchs K., Mastin L., Gregersen S., Pavoni N., Stephansson O. and Ljunggren C., 1992. Regional patterns of tectonic stress in Europe. *J. Geophys. Res.*, **97(B8)**, 11783−11803.

Nehybka V. and Skácelová Z., 1995. Seismotectonic analysis of the seismological measurements in the Kraslice network. *Věstník Českého geologického ústavu*, **70**, 97−100.

Nishizawa O., 1982. Seismic velocity anisotropy in a medium containing oriented cracks - transversely isotropic case. *J. Phys. Earth*, **30**, 331−347.

Okaya D., Rabbel W., Beilecke T. and Hasenclever J., 2004. P wave material anisotropy of tectono-metaorphic terrane: An active source seismic exoeriment at the KTB super-deep drill hole, southeast Germany. *Geophys. Res. Lett.*, **31**, L24620, doi: 10.1029/2004GL020855.

Peacock S. and Hudson J.A., 1990. Seismic properties of rocks with distributions of small cracks. *Geophys. J. Int.*, **102**, 471–484.

Peška P., 1992. Stress indications in the Bohemian Massif: Reinterpretation of borehole televiewer data. *Stud. Geophys. Geod.*, **36**, 307–324.

Plomerová J., Achauer U., Babuška V., Vecsey L. and BOHEMA working group, 2007. Upper mantle beneath the Eger Rift (Central Europe): plume or asthenosphere upwelling? *Geophys. J. Int.*, **169**, 675−682, doi: 10.1111/j.1365-246X.2007.03361.x.

Pros Z., Lokajíček T., Přikryl R., Špičák A., Vajdová V. and Klíma K., 1998. Elastic parameters of West Bohemian granites under hydrostatic pressure. *Pure Appl. Geophys.*, **151**, 631−646.

Rabbel W., 1994. Seismic anisotropy at the Continental Deep Drilling site (Germany). *Tectonophysics*, **232**, 329–341.

Rabbel W., Beilecke T., Bohlen T., Fischer D., Frank A., Hasenclever J., Borm G., Kück J., Bram K., Druivenga G., Lüschen E., Gebrande H., Pujol J. and Smithson S., 2004. Superdeep vertical seismic profiling at the KTB deep drill hole (Germany): Seismic close-up view of a major thrust zone down to 8.5 km depth. *J. Geophys. Res.*, **109**, B09309, doi: 10.1029/2004JB002975.

Rabbel W. and Mooney W.D.F., 1996. Seismic anisotropy of the crystalline crust: what does it tell us? *Terra Nova*, **8**, 16–21.

Rössler D., Rümpker G. and Krüger F., 2004. Ambiguous moment tensors and radiation patterns in anisotropic media with applications to the modeling of earthquake mechanisms in W-Bohemia. *Stud. Geophys. Geod.*, **48**, 233–250.

Rössler D., Krüger F. and Rümpker G., 2007. Retrieval of moment tensors due to dislocation point sources in anisotropic media using standard techniques. *Geophys. J. Int.*, **169**, 136–148.

Růžek B., Vavryčuk V., Hrubcová P., Zedník J. and Celebration Working Group, 2003. Crustal anisotropy in the Bohemian Massif, Czech Republic: Observations based on Central European Lithospheric Experiment Based on Refraction (CELEBRATION) 2000. *J. Geophys. Res.*, **108**, 2392, doi: 10.1029/2002JB002242.

Savage M.K., 1999. Seismic anisotropy and mantle deformation: what have we learned from shear wave splitting? *Rev. Geophys.*, **37**, 65–16.

Vavryčuk V., 1993. Crustal anisotropy from local observations of shear-wave splitting in West Bohemia, Czech Republic. *Bull. Seismol. Soc. Amer.*, **83**, 1420–1441.

Vavryčuk V., 1995. Reply to comments on “Crustal anisotropy from local observations of shear-wave splitting in West Bohemia, Czech Republic” by Bokelmann G.H.R. and Kawahara J.: Can the Hudson crack model describe behavior of real cracks? *Bull. Seismol. Soc. Amer.*, **85**, 661–664.

Vavryčuk V., 2002. Non-double-couple earthquakes of January 1997 in West Bohemia, Czech Republic: Evidence of tensile faulting. *Geophys. J. Int.*, **149**, 364–373, doi: 10.1046/j.1365-246X.2002.01654.x.

Vavryčuk V., Hrubcová A., Brož M., Málek J. and ALP 2002 Working Group, 2004. Azimuthal variation of Pg velocity in the Moldanubian, Czech Republic: Observations based on a multi-azimuthal common-shot experiment. *Tectonophysics*, **387**, 189–203, doi: 10.1016/j.tecto.2004.06.015.

Vavryčuk V., 2005. Focal mechanisms in anisotropic media. *Geophys. J. Int.*, **161**, 334–346, doi: 10.1111/j.1365-246X.2005.02585.x.

Vavryčuk V., 2006. Focal mechanisms produced by shear faulting in weakly transversely isotropic crustal rocks. *Geophysics*, **71**, D145–D152, doi: 10.1190/1.2236378.

Wirth W., Plenefisch T., Klinge K., Stammler K. and Seidl D., 2000. Focal mechanisms and stress field in the region Vogtland/Western Bohemia. *Stud. Geophys. Geod.*, **44**, 126–141.